DEVELOPMENTAL DYNAMICS 214:55–65 (1999)

Spatial and Temporal Changes in Chondroitin Sulfate Distribution in the Sclerotome Play an Essential Role in the Formation of Migration Patterns of Mouse Neural Crest Cells

YUKIHIKO KUBOTA,[1] TOSHITERU MORITA,[1] MORIAKI KUSAKABE,[2] TERUYO SAKAKURA,[3] AND KAZUO ITO[1]*

[1]*Department of Biology, Graduate School of Science, Osaka University, Osaka, Japan*
[2]*Division of Experimental Animal Research, RIKEN, Tsukuba, Japan*
[3]*Department of Pathology, School of Medicine, Mie University, Mie, Japan*

ABSTRACT **We have examined the roles of pertinent extracellular matrix molecules in the formation of the neural crest cell migration patterns in the sclerotome of the mouse embryo. The present data indicate that permissiveness for migration is inversely correlated with chondroitin sulfate content. Experimental removal of chondroitin sulfate proteoglycans in the embryo causes neural crest cells to migrate even within the posterior half of the somite, which they do not invade ordinarily. Moreover, three different sclerotomal regions defined by the presence or absence of the ventromedial and/or ventrolateral pathways are present along the anteroposterior axis and undergo systematic temporal changes that affect migration patterns. The most anterior portion of the sclerotome is conducive to both ventromedial and ventrolateral migration (Anterior Region). The intermediate portion is conducive to ventromedial migration only (Intermediate Region). No neural crest cells are seen within the posterior portion of the sclerotome (Posterior Region). At this level, they are observed exclusively in the dorsolateral space adjacent to the roof of the neural tube. With advancing embryonic development, the rostrocaudal length of the Anterior Region decreases and is accompanied by a corresponding enlargement of the Intermediate Region. These results suggest that temporal and regional differences in the sclerotome contribute to the neural crest cell migration patterns in the mouse. To refine our understanding of the underlying mechanisms, regional differences and temporal changes in the distribution of extracellular matrix molecules have been examined during migration. In the sclerotome, chondroitin sulfate displays distinct distribution patterns that are closely correlated with the migration patterns of mouse neural crest cells. Furthermore, their migration patterns are altered in embryos treated with the inhibitors of chondroitin sulfate proteoglycan biosynthesis, sodium chlorate, and β-D-xyloside. In inhibitor-treated embryos, neural crest cell migration occurs even in the posterior portion of the sclerotome. The metameric organization of dorsal root ganglia is disturbed in these embryos. Our observations provide novel evidence for the importance of sclerotomal chondroitin sulfate distribution patterns in mouse crest cell migration patterns. We conclude that systematic spatiotemporal changes in the distribution of chondroitin sulfate proteoglycans are a key requisite for the formation of migration patterns of mouse neural crest cells in the sclerotome.** ***Dev Dyn 1999;214:55–65.***

Key words: migration patterns; mouse neural crest cells; chondroitin sulfate; sodium chlorate; β-D-xyloside

INTRODUCTION

Neural crest cells emigrate from the neural tube. They migrate ventrally and laterally and give rise to a variety of derivatives, including melanocytes, peripheral nerve cells and their supporting cells, and ectomesenchymal cells in vertebrate embryos (Weston, 1970; Le Douarin, 1982; Hall, 1988). In the trunk region of the amniote embryo, the cells migrate along two predominant pathways (Weston, 1963; Le Douarin, 1973; Erickson et al., 1989; Hou and Takeuchi, 1994): 1) the dorsolateral pathway between the dermomyotome and the epidermis (Serbedzija et al., 1989, 1990; Kubota et al., 1996) and 2) the ventral pathway through the anterior half of the somite (Rickmann et al., 1985; Bronner-Fraser, 1986; Kubota et al., 1996). Furthermore, two different types of ventral routes have been found in the anterior half, that is, the ventromedial

Grant sponsor: Grants-in-Aid for Scientific Research from Ministry of Education, Science and Culture of Japan (K.I.); Grant number: 08680791.
*Correspondence to: Dr. Kazuo Ito, Department of Biology, Graduate School of Science, Osaka University, 1-16 Machikaneyama, Toyonaka, Osaka 560-0043, Japan. E-mail: itokazuo@bio.sci.osaka-u.ac.jp
Received 18 May 1998; Accepted 9 October 1998

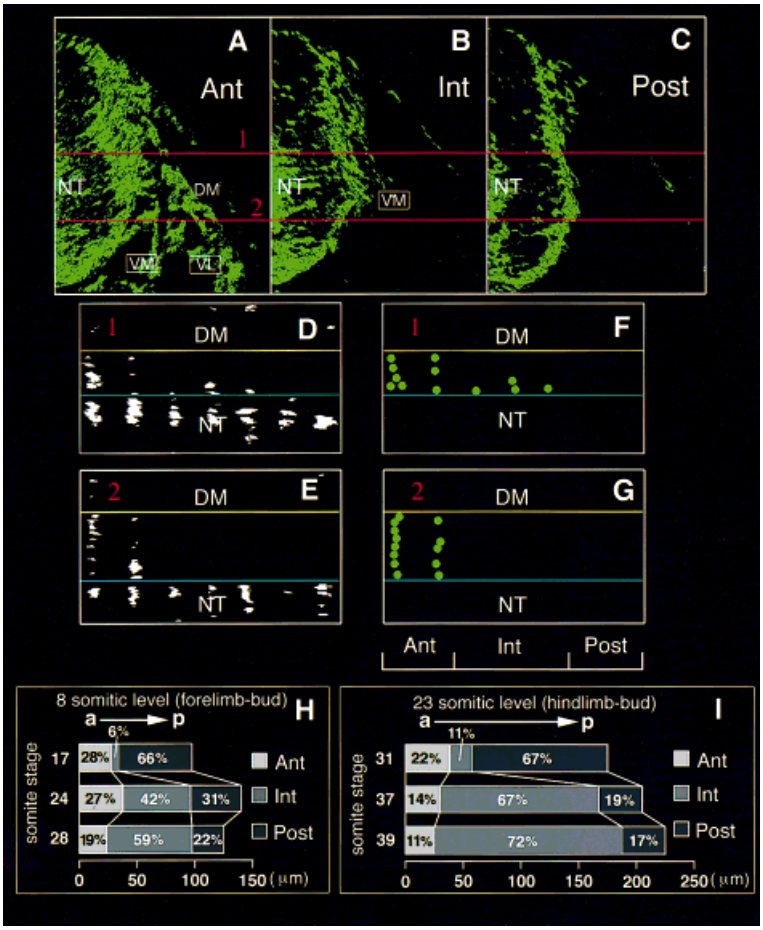

Fig. 1. Three-dimensional analysis of migration patterns of 4E9R-positive neural crest cells in the sclerotome at the 8 somitic level of 24 somite embryo (intermediate migratory stage). Transverse cryosections were double-stained with 4E9R and antilaminin. Antilaminin was used to elucidate the borders between the dermomyotome and sclerotome and between the sclerotome and neural tube. **A–C:** Neural crest cell distribution in transverse images of the Anterior (A), Intermediate (B), and Posterior (C) Regions sliced from the three-dimensional somitic reconstruction. **D–G:** Distribution of 4E9R-specific signals in horizontal slices of the same reconstructed image. The reconstructed image was horizontally sliced at levels 1 and 2 (red lines) in Figs. A–C. Yellow and blue lines show the boundaries between the dermomyotome and sclerotome and between the sclerotome and neural tube, respectively. Neural crest cell-specific signals in Figs. D and E are schematically indicated as green dots in Figs. F and G, respectively. **H, I:** Rostrocaudal length of the Anterior, Intermediate, and Posterior Regions. Estimation was performed using 4 or 6 embryos. a, anterior; p, posterior; Ant, Anterior Region; Int, Intermediate Region; Post, Posterior Region; DM, dermomyotome; NT, neural tube; VL, ventrolateral pathway; VM, ventromedial pathway.

pathway along the medial portion of the sclerotome (Serbedzija et al., 1990; Kubota et al., 1996) and the ventrolateral pathway along the lateral portion of the sclerotome (Loring and Erickson, 1987; Serbedzija et al., 1990; Tosney et al., 1994; Kubota et al., 1996).

Specific neural crest derivatives differentiate in precise embryonic locations. For instance, the peripheral autonomic and spinal sensory ganglia are derived from neural crest cells that migrate along the ventral pathway and organized in a segmented pattern (Keynes and Stern, 1984, 1988; Kalcheim and Teillet, 1989; Goldstein et al., 1990). Neural crest cell migration along the ventral route might be spatially and temporally regulated even in the anterior half of the sclerotome, in order to generate peripheral ganglia in defined locations. Careful examination of spatial and temporal changes in neural crest cell migration (migration patterns) will provide valuable data for analyzing what mechanisms are involved in the formation of migration patterns.

Whereas the laboratory mouse has been used extensively for genetic studies of neural crest development (Silvers, 1979; Erickson and Weston, 1983; Sternberg and Kimber, 1986; Morrison-Graham and Weston, 1989; George et al., 1993; Lo et al., 1994; Schuchardt et al., 1994), less is known about the mechanisms underlying migration patterns of mouse neural crest cells. We have therefore examined by three-dimensional image analysis the migration patterns of mouse neural crest cells translocating along the ventral pathway using the mouse neural crest cell-specific antibody, 4E9R (Kubota et al., 1996), and focused on regional differences and temporal changes in the sclerotomal distribution of extracellular matrix molecules as one of mechanisms underlying their migration patterns. Our data demonstrate that the migration of mouse neural crest cells is spatially and temporally regulated even in the anterior half of the sclerotome and that the migration patterns are closely correlated with distribution patterns of sclerotomal chondroitin sulfate. Experiments using the inhibitors of chondroitin sulfate proteoglycan synthesis indicate that altering sclerotomal chondroitin sulfate proteoglycan content changes the migration patterns of mouse neural crest cells.

RESULTS

Spatiotemporal Changes in Neural Crest Cell Migration in the Sclerotome

In order to analyze regional differences in the migration of mouse neural crest cells in the sclerotome in

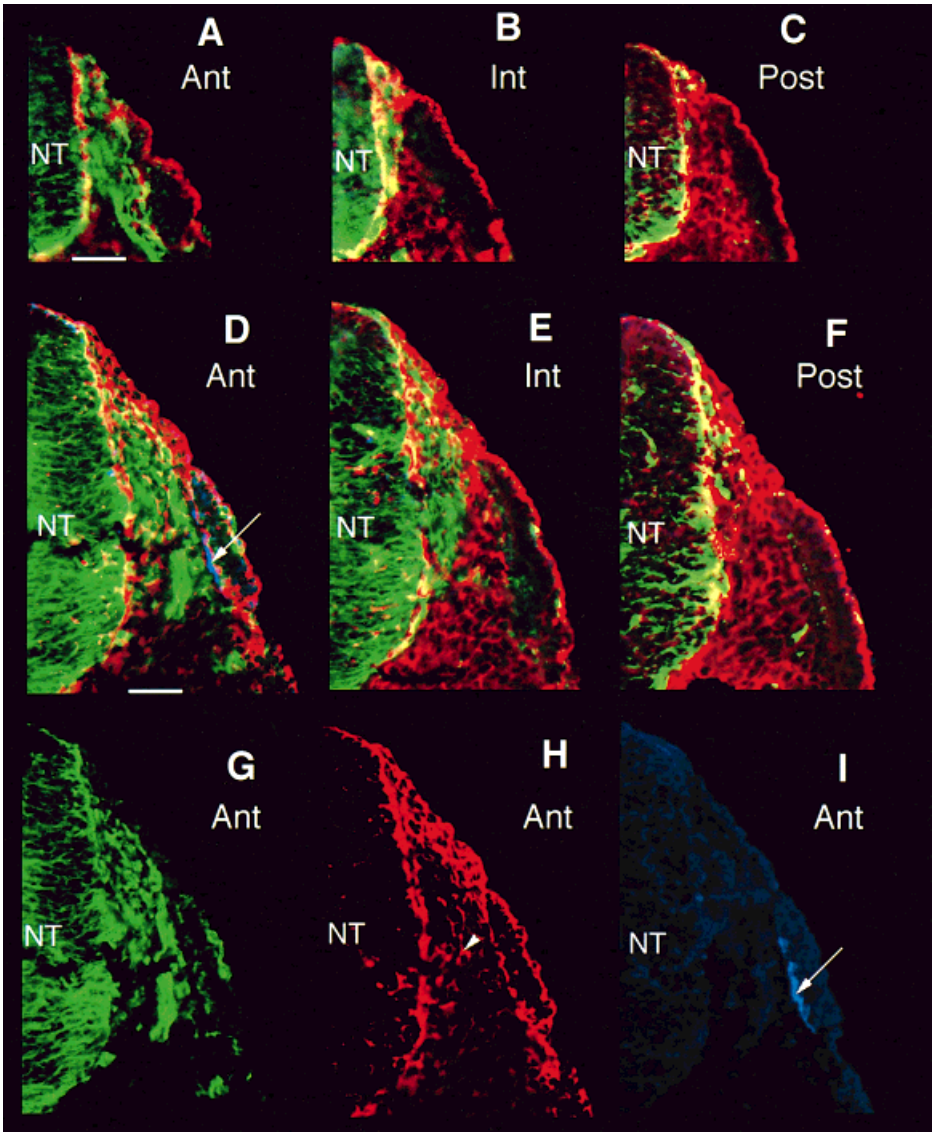

Fig. 2. Distribution of neural crest cells (green), chondroitin sulfate (CS; red) and tenascin (TN; blue) in sections triple-stained. **A–C:** Transverse sections of the Anterior (A), Intermediate (B), and Posterior (C) Regions at the 8 somitic level of 24 somite embryo (intermediate migratory stage). CS is not observed in the Anterior Region (A). TN is not found. **D–I:** Transverse sections of the Anterior (D, G–I), Intermediate (E), and Posterior (F) Regions at the 8 somitic level of 28 somite embryo (late migratory stage). Figures G, H, and I show the distribution of neural crest cells, CS and TN in the same region as in Fig. D. CS begins to be found in the dorsal portion of the Anterior Region (arrowhead in Fig. H). TN is observed in the boundary between the dermomyotome and sclerotome in the Anterior Region (arrows in Figs. D and I). Ant, Anterior Region; Int, Intermediate Region; Post, Posterior Region; NT, neural tube. Bars: 50 μm.

detail, we made three-dimensional somitic reconstructions of serial transverse cryosections immunostained with 4E9R and antilaminin and examined the distribution of neural crest cells in various slices of the reconstructed images. Three different sclerotomal regions defined by the presence or absence of the ventromedial and/or ventrolateral pathways were arranged along the anteroposterior axis. In the most anterior portion of the sclerotome, both ventromedial and ventrolateral pathways were observed (Anterior Region; Fig. 1A). In the intermediate portion following the Anterior Region, the ventromedial route was present only (Intermediate Region; Fig. 1B). No neural crest cells were seen in the posterior portion of the sclerotome (Posterior Region; Fig. 1C). Neural crest cells were observed ubiquitously in the dorsolateral space adjacent to the roof of the neural tube (Fig. 1A–C). These regional differences in neural crest cell distribution in the sclerotome were confirmed in horizontal slices of the somite. In the Anterior Region, streams of neural crest cells along the ventromedial pathway as well as the ventrolateral route extended to the level of the sympathetic nerve plexus (Fig. 1A,D–G). Equivalent cells in the Intermediate Region were observed as far as the dorsal root

ganglionic region (Fig. 1B,D–G). These regional differences in neural crest cell distribution were similar at the forelimb-bud (8 somitic levels) and hindlimb-bud (23 somitic levels) levels.

The rostrocaudal length of the Anterior, Intermediate, and Posterior Regions was estimated by the number of 2-μm-thick serial transverse optical sections covering each region, in order to indicate temporal changes in the regional size during neural crest cell migration. The extent of the Intermediate Region increased at the expense of the Anterior and Posterior Regions, both of which decreased in length with progressing embryogenesis (Fig. 1H,I).

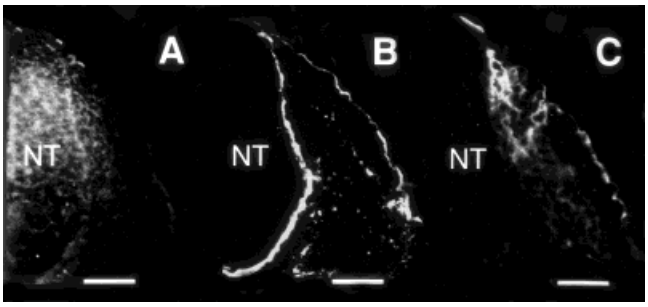

Fig. 3. Distribution of dermatan sulfate (**A**), perlecan (**B**), and keratan sulfate (**C**) in the Anterior Region at the 8 somitic levels of 25 somite embryos (intermediate migratory stage). NT, neural tube. Bars: 50 μm.

Distribution of Extracellular Matrix Molecules During Neural Crest Cell Migration

The distribution of extracellular matrix materials was immunohistochemically examined to explore their role in the formation of migration patterns of neural crest cells. Rostrocaudal differences in sclerotomal CS-56-positive chondroitin sulfate (CS) distribution were observed during neural crest cell migration. While a clear CS signal was not found in the Anterior Region (Fig. 2A), it appeared in the Intermediate and Posterior Regions (Fig. 2B,C). In the Intermediate Region, however, CS was reduced in the ventromedial pathway (Fig. 2B). CS content increased with advancing cell migration, possibly explaining the decrease in rostrocaudal length of the Anterior Region. At the late migratory stage (8 somitic levels of 28 somite stage embryos or 23 somitic levels of 39 somite stage embryos), there was a gradual increase in CS in the dorsal portion of the Anterior Region (Fig. 2A,D,H). Furthermore, neural crest cells started to accumulate in the dorsal root ganglionic region within the Intermediate Region. CS was absent in the presumptive ganglion (Fig. 2E). Again, these changes were similar at both the forelimb-bud and hindlimb-bud levels. CS in the sclerotome disappeared in tissue sections treated with chondroitinase ABC and chondroitinase AC II.

Laminin (LN) was observed in the basement membrane. The boundary between the dermomyotome and sclerotome showed intense LN-immunoreactivity at the intermediate migratory stage (8 somitic levels of 24–25 somite stage embryos or 23 somitic levels of 37 somite stage embryos). At all stages and axial levels examined, fibronectin (FN) was uniformly distributed in the sclerotome. No regional differences in the distribution of LN and FN were detected in the sclerotome. The distribution of tenascin (TN) was more restricted both spatially and temporally. TN immunoreactivity in the sclerotome was only observed in the Anterior Region of the late migratory stage (Fig. 2D–F,I). TN was localized in the ventral portions of boundaries containing LN between adjacent dermomyotomes and between the sclerotome and dermomyotome (Fig. 2D,I).

The spatial and temporal localization of dermatan sulfate (DS), heparan sulfate (HS), and keratan sulfate (KS) does not correlate with neural crest cell migration patterns in the sclerotome. 2B6-positive DS appeared in the subepidermal space at the early migratory stage (8 somitic levels of 17 somite stage embryos or 23 somitic levels of 31 somite stage embryos). DS was observed in the dorsolateral space adjacent to the neural tube and in the dorsal portion of the sclerotome and neural tube after the intermediate migratory stage (Fig. 3A). HK-102-immunoreactive perlecan (core protein of heparan sulfate proteoglycan) and 10E4-positive HS were localized in the basement membrane around the neural tube and notochord and beneath the epidermis (Fig. 3B). HS disappeared in sections treated with heparitinase. 5D4-immunoreactive KS was found initially in the subepidermal basement membrane. At the intermediate migratory stage, KS appeared in the dorsolateral space adjacent to the neural tube (Fig. 3C). It was observed in the perinotochordal space at the late migratory stage.

Migration Patterns of Neural Crest Cells in Embryos Treated With Sodium Chlorate or β-D-Xyloside

Since progressive changes in the sclerotomal distribution of CS are likely to be correlated with the neural crest cell migration patterns, the role of CS in the formation of their migration patterns was analyzed in embryos treated with sodium chlorate or β-D-xyloside to perturb CS distribution. In treated embryos, the average of one-somite length was 130 ± 0.6 μm at the 24–25 somite stages. It was similar to the average one-somite length in control (PBS- or α-D-xyloside-treated) embryos (125 ± 1.3 μm). Of embryos (9/89) treated with 40.0 (3/25) or 10.6 mg (2/21) sodium chlorate, or with 5.0 mg β-D-xyloside (4/43), 10% showed incomplete closure of the neural tube at cranial and/or rostral trunk levels. Neural crest cell emigration occurred even in axial levels where incomplete neural tube closure was found. Of the treated embryos, 90% (38/43) were viable at embryonic day (Ed) 11.0 (26/30) and Ed 11.5 (12/13).

In treated embryos, neural crest cells invaded the sclerotome not only in the anterior (Fig. 4A,E) and intermediate portions (Fig. 4B,F) but also in the posterior portion (Fig. 4C,G) of the somite. In the anterior portion, ventrolateral and ventromedial pathways appeared and extended ventrally to the level of the sympathetic nerve plexus (Fig. 4A,E). Neural crest cell migration in this portion was similar to that in the Anterior Regions in control embryos (Fig. 1A). The intermediate portion was conducive to ventromedial migration only (Fig. 4B,F). The rostrocaudal length of the anterior and intermediate portions (Fig. 4K) was comparable to that of the Anterior and Intermediate Regions in control embryos (Fig. 1H). The ventromedial pathway in the intermediate portion reached the level of the sympathetic nerve plexus in contrast to control embryos (Fig. 1B). Ventrolateral-like and ventromedial-like pathways were observed in the posterior portion (Fig. 4C,G). The distribution of neural crest cells in these pathways expanded into the level of the sympathetic nerve plexus. The alteration of neural crest cell migration patterns was similar with both 12- and 24-hour treatments.

The staining intensity of CS in treated embryos (Fig. 4A–C,E–G) was reduced in the entire sclerotome compared to control embryos (Fig. 4D,H). When brief digestion of CS (chondroitinase ABC treatment for 10 minutes) was performed in cryosections from embryos treated with sodium chlorate, the intensity of 1B5-positive unsulfated chondroitin in the sclerotome was higher in sodium chlorate-treated (Fig. 4I) than in control embryos (Fig. 4J). Unsulfated chondroitin around the notochord was observed in both sodium chlorate-treated and control embryos. The distribution of LN (Fig. 4A–C,E–G) and FN in the sclerotome was similar to that in control embryos (Fig. 4D,H). TN in the anterior portion of the sclerotome at the forelimb-bud level appeared after the 28 somite stage only. The timing of TN expression and its localization were also similar to those in control embryos. The observation that TN distribution is restricted in the anterior portion confirms that the rostrocaudal polarity of the somite is unchanged in treated embryos. HS and perlecan were localized in the basement membrane. KS was found in the subepidermal basement membrane and in the dorsolateral space adjacent to the neural tube. DS appeared in the subepidermal and dorsolateral space and in the dorsal sclerotome and dorsal neural tube. Again, the distribution of HS (and perlecan), KS and DS was similar to that in control embryos. The immunoreactivity of DS, but not KS and HS, was slightly weaker in treated embryos.

The alteration of neural crest cell migration in the sclerotome of treated embryos may affect the organization of neural crest derivatives. Therefore, we examined the organization of dorsal root ganglia (DRG) in treated embryos. Whereas the segmented organization of DRG was observed in control embryos (Fig. 5A,B,E), DRG appeared even in the most caudal level of the sclerotome in treated embryos (Fig. 5D). In horizontal sections stained with 40.2D6 (anti-Islet-1 homeobox protein) or NR-4 (antineurofilament 68 kDa), there was abnormal DRG segmentation, as adjacent DRG combined, in treated embryos (Fig. 5F–H). Immunoreactivity of DRG neurons to 40.2D6 and NR-4 was comparable in treated and control embryos.

DISCUSSION

Migration Patterns of Mouse Neural Crest Cells in the Sclerotome

It has been shown that mouse neural crest cells enter the anterior half of the somite and migrate along the ventromedial and ventrolateral pathways (Serbedzija et al., 1990; Kubota et al., 1996). The present data extend results obtained in these previous studies. The Anterior Region is conducive to both ventrolateral and ventromedial migration. The Intermediate Region is permissive to ventromedial migration only. The rostrocaudal extent of the Anterior Region decreases and is accompanied by an enlargement of the Intermediate Region with advancing migration. These data show that neural crest cell migration differs between the rostral (Anterior Region) and caudal (Intermediate Region) portions in the anterior half of the somite and that there is a progressive change in the size of the regions that are permissive to migration.

Serbedzija et al. (1990) have suggested that two overlapping migratory phases of mouse neural crest cells are at the forelimb-bud level: 1) an early ventrolateral pathway which opens by Ed 9.0 and closes by Ed 9.5, and 2) a later ventromedial pathway which appears after Ed 9.0–9.5. Our data are in agreement with this model. During early migration at the forelimb-bud level (17 somite stage; Ed 9.0), neural crest cells migrate primarily in the Anterior Region where the ventrolateral pathway is present. The extent of this region decreases at the 28 somite stage (late Ed 9.5). The Intermediate Region, which is conducive to ventromedial migration only, expands with advancing migration and occupies the majority of the sclerotome by late Ed 9.5. These results suggest that migration along the ventrolateral pathway terminates by late Ed 9.5 and that most of the later emigrating crest cells take the ventromedial pathway at the forelimb-bud level.

We found that streams of neural crest cells extend ventrally to the level of the sympathetic nerve plexus in the Anterior Region. By contrast, most neural crest cells in the Intermediate Region are distributed as far as the DRG level. Our observations thus suggest that early emigrating neural crest cells migrating in the Anterior Region populate the DRG or the sympathetic nerve chain and a later migrating group of cells in the Intermediate Region colonizes exclusively the DRG. Taken together, our data indicate that the regional differences and temporal changes within the sclerotome generate the migration patterns of mouse neural crest cells.

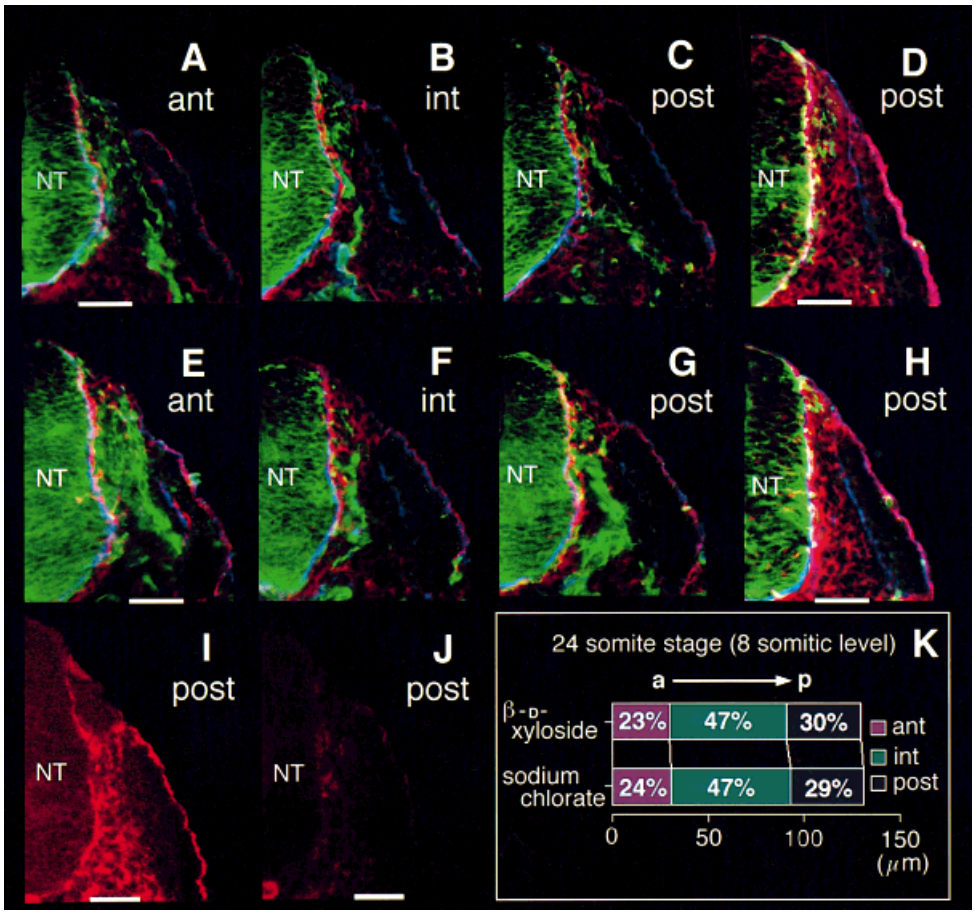

Fig. 4. Distribution of neural crest cells (green), chondroitin sulfate (red) and laminin (blue) at the 8 somitic levels of 24 somite embryos treated with β-D-xyloside or with sodium chlorate for 12 hours. **A–C:** Transverse sections of the anterior (A), intermediate (B), and posterior (C) portions of the sclerotome in the embryo treated with 5 mg β-D-xyloside. **D:** Transverse section of the posterior portion of the sclerotome in the embryo treated with 5 mg α-D-xyloside for 12 hours. **E–G:** Transverse sections of the anterior (E), intermediate (F), and posterior (G) portions of the sclerotome in the embryo treated with 40 mg sodium chlorate. **H:** Transverse section of the posterior portion of the sclerotome in the embryo treated with PBS for 12 hours. **I, J:** IB5-positive unsulfated chondroitin in posterior portions of the sclerotome at the 8 somitic levels of 25 somite embryos treated with 40 mg sodium chlorate (I) or PBS (J). **K:** Rostrocaudal length of the anterior, intermediate, and posterior portions of the sclerotome in the embryos treated with β-D-xyloside or sodium chlorate. Estimation was performed using 5 embryos, respectively. a, anterior; p, posterior; ant, anterior portion; int, intermediate portion; post, posterior portion; NT, neural tube. Bars: 50 μm.

Chondroitin Sulfate Is Essential for Pattern Formation of Mouse Neural Crest Cell Migration in the Sclerotome

The present study shows that CS is present in the sclerotome during all migratory stages of mouse neural crest cells. This is in agreement with the previous data from other investigators (Weston et al., 1977; Derby, 1978; Trasler and Morriss-Kay, 1991). The present data furthermore show that sclerotomal CS is distributed exclusively in the regions where neural crest cells do not migrate. It has been shown that CS-containing materials are distributed in the posterior half of the avian sclerotome (Newgreen et al., 1990; Oakley and Tosney, 1991; Landolt et al., 1995) and inhibit neural crest cell migration (Tan et al., 1987; Perris et al., 1996; Kerr and Newgreen, 1997). Sclerotomal CS may play an important role in the restriction of regions permissive to mouse neural crest cell migration. We found that regional and temporal differences in sclerotomal CS distribution are closely correlated with neural crest cell migration patterns (Fig. 6). Our results thus suggest that systematic spatiotemporal changes in CS distribution in the sclerotome contribute to the formation of migration patterns of neural crest cells by restricting the regions conducive to migration.

The idea that dynamic changes in sclerotomal CS distribution are an underlying mechanism for regulating migration patterns of mouse neural crest cells is supported by our data from experiments with specific inhibitors of sulfated proteoglycan synthesis. In inhibi-

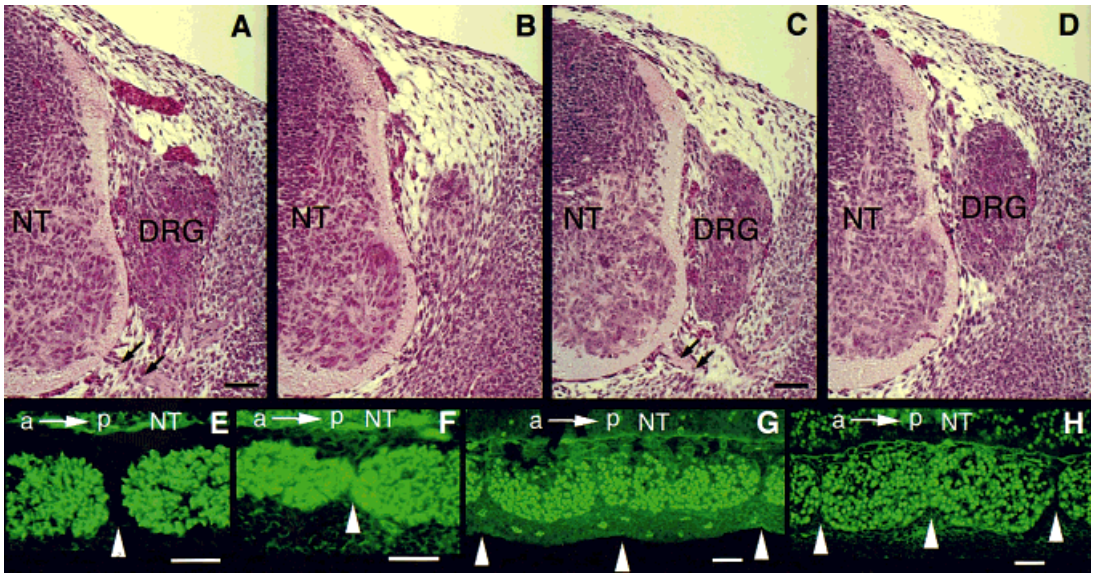

Fig. 5. Organization of dorsal root ganglia at the forelimb-bud levels of control **(A, B, E)** and 40 mg sodium chlorate-treated **(C, D, F–H)** embryos. A–D: Transverse sections at rostral (A, C) and caudal (B, D) levels of the sclerotome in embryonic day (Ed) 11.5 embryos. Motor axons (arrows in Figs. A and C) are observed in rostral portions of the sclerotome. E–H: Horizontal sections of Ed 11.0 (E–G) and Ed 11.5 (H) embryos. (E, F) Antineurofilament 68kDa staining. (G, H) Anti-Islet-1 staining. Arrowheads indicate boundaries between somitic segments. a, anterior; p, posterior; DRG, dorsal root ganglion; NT, neural tube. Bars: 50 μm.

tor-treated embryos, neural crest cells invade the posterior portion of the sclerotome in addition to the anterior and intermediate portions. This alteration of the migration patterns occurs concomitantly with the reduction in sclerotomal CS. A significant reduction of HS, KS, and DS was not observed in treated embryos, indicating that CS is the main component that is disrupted in these embryos during neural crest cell migration. Sodium chlorate is a specific inhibitor of sulfation, causing under-sulfation of sulfated proteoglycans (Farley et al., 1978). The increase of sclerotomal 1B5-positive unsulfated chondroitin in sodium chlorate-treated embryos shows that under-sulfation of sclerotomal CS occurs in embryos treated with this inhibitor by a intraperitoneal injection. β-D-Xyloside competes with protein-bound xylose for galactosyl transferase, and thereby brings about a reduction in the level of protein-bound sulfated proteoglycan synthesis (Schwartz et al., 1974; Schwartz, 1977). In intact chicken embryos, normal synthesis of chondroitin sulfate proteoglycans (CS-PGs) was disturbed by this compound (Oohira et al., 1981). Furthermore, α-anomer of β-D-xyloside (α-D-xyloside) has no effects on CS content. Thus, both substances inhibit normal biosynthesis of CS-PGs in experimental condi-

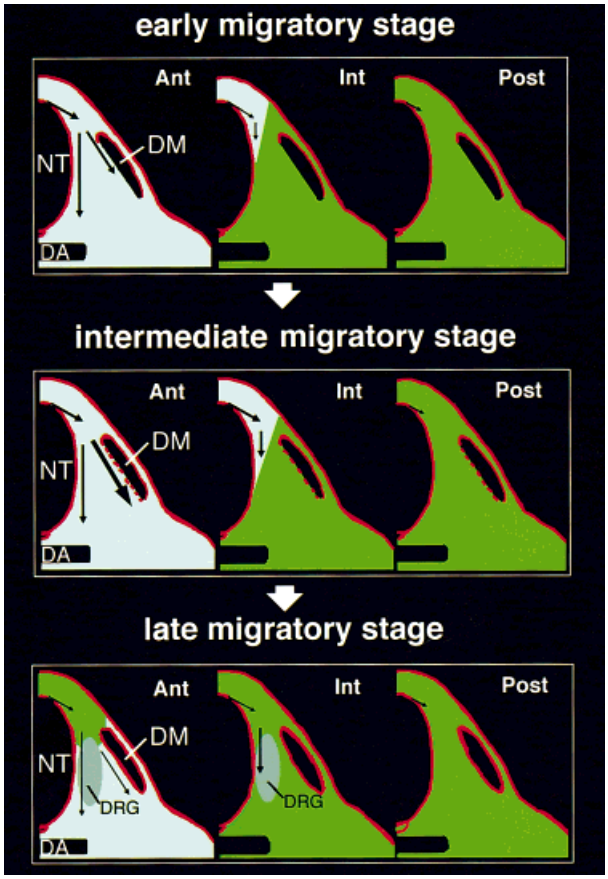

Fig. 6. Schematic diagram of regional and temporal differences in the mouse sclerotome. Arrows indicate the migratory pathways of neural crest cells. Green, chondroitin sulfate (CS)-rich region; light green, CS-poor region; red, laminin-containing basement membrane. Ant, Anterior Region; Int, Intermediate Region; Post, Posterior Region; DA, dorsal aorta; DM, dermomyotome; DRG, dorsal root ganglion; NT, neural tube.

tions used in this study and accordingly interfere with normal distribution of CS-PGs as suggested by previous studies (Morriss-Kay and Crutch, 1982; Davies et al., 1995; Kispert et al., 1996). We therefore conclude that the alteration of neural crest cell migration patterns in treated embryos is due to disturbances in sclerotomal CS-PGs distribution. The metameric organization of DRG was disordered in treated embryos, showing that this alternation affects their segmentation.

Ventrolateral and/or ventromedial pathways appear in the anterior or intermediate sclerotome of inhibitor-treated embryos, while a reduction in CS occurs in the entire sclerotome. It is conceivable that other cues contribute to forming the specific migratory pathways. It has been shown that neural crest cell migration is directed by interactions between receptor tyrosine kinases and their ligands (Wehrle-Haller and Weston, 1995, 1997; Krull et al., 1997; Wang and Anderson, 1997). Distinct subpopulations of neural crest cells express specific receptor tyrosine kinases (Kahane and Kalcheim, 1994; Henion et al., 1995; Wehrle-Haller and Weston, 1997). A gradient of ligand released from the target tissue might guide neural crest cell subpopulations into their specific target organ by chemotaxis (Wehrle-Haller and Weston, 1997). It is possible that neural crest cell migration patterns are determined by both distinct sclerotomal CS-PGs distribution that restricts the regions permissive to migration and chemotactic guidance that generates specific migratory pathways in the regions.

The distribution patterns of CS in the mouse sclerotome are comparable to those of proteoglycans containing CS and KS (CS/KS-PGs), such as PG-H/aggrecan (Oike et al., 1980; Perris et al., 1996), in the chicken sclerotome (Perris et al., 1991). However, the distribution of 5D4-positive KS, which colocalized with CS in the chicken sclerotome, differs from that of CS in the mouse sclerotome. DS and HS distribution also differ from CS. CS-PG isolated from the quail trunk lacks KS, HS, and DS and influences neural crest cell behavior (Kerr and Newgreen, 1997). CS-PGs, which change spatiotemporally in the mouse sclerotome, appear to be CS-PGs possibly lacking KS, HS, and DS. Taken together, these observations indicate that spatial and temporal changes in sclerotomal CS-PGs expression are an underlying mechanism for regulating migration patterns of mouse neural crest cells.

EXPERIMENTAL PROCEDURES

Immunohistochemistry and Histology

ddY strain mice were used. Embryos were staged by scoring the number of somites. Immunohistochemistry was performed as described previously (Kubota et al., 1996). Mouse embryos were fixed with methanol containing 0.1% formaldehyde for 10–20 minutes at −20°C. For immunostainings with 40.2D6 (anti-Islet-1), embryos were fixed in 4% paraformaldehyde in phosphate-buffered saline (PBS, pH 7.4) for 12 hours on ice. For immunolabelings with NR-4 (antineurofilament 68 kDa), embryos were fixed in 10% formalin in PBS for 10 minutes at room temperature and subsequently in methanol at −20°C. Fixed embryos were immersed in gradually increasing sucrose solutions and embedded in OCT compound (Miles). Cryostat sections were serially cut at 10–20 μm and mounted on albumin-coated glass slides. The primary and secondary antibodies that were used are listed in Table 1. With the exception of CS-56 and 2B6, primary antibodies were applied to cryosections for 12 hours at 4°C. CS-56 and 2B6 were used for 30 minutes and for 2 hours at room temperature, respectively. Sections were treated with secondary antibodies for 1 hour at room temperature. Routine histological methods were employed. Embryos were fixed with Bouin's fixative and embedded in paraffin (Oxford Laboratory). Serial transverse sections were cut at 7 μm and stained with hematoxylin and eosin.

Enzyme Treatment

Cryosections were treated with 0.1 U/ml chondroitinase ABC (Seikagaku Corp.) in 0.1 M Tris-HCl buffer (pH 8.0) containing 30 mM sodium acetate and 10 mM EDTA for 10–30 minutes at 37°C (Yada et al., 1996) or 0.2 U/ml chondroitinase AC II Arthro (Seikagaku Corp.) in 0.1 M Tris-HCl buffer (pH 6.0) containing 30 mM sodium acetate for 2 hours at 37°C (Perris et al., 1991). Chondroitinase B (Seikagaku Corp.) was applied to sections at a concentration of 10 mU/ml in 0.1 M Tris-HCl buffer (pH 8.0) containing 30 mM sodium acetate, 10 mM EDTA and protease inhibitors (2 mM PMSF, 2 μg/ml pepstatin A, 20 μg/ml leupeptin) for 30–60 minutes at 30°C (Sobue et al., 1989). Heparitinase (Seikagaku Corp.) was used at 5 mU/ml in 50 mM Hepes buffer (pH 7.0) containing 100 mM sodium chloride, 1 mM calcium chloride, 5 μg/ml of BSA, and protease inhibitors for 2 hours at 37°C (David et al., 1992).

Sodium Chlorate and β-D-Xyloside Treatment

Two specific inhibitors of sulfated proteoglycan synthesis (Okayama et al., 1973; Schwartz, 1977; Farley et al., 1978), β-D-xyloside (p-nitrophenyl β-D-xylopyranoside; Nakarai Tesque Inc.) and sodium chlorate (Nakarai Tesque Inc.), were used in this study. Both substances were dissolved in PBS; 5, 1.0, or 0.3 mg/mouse of β-D-xyloside was intraperitoneally injected into pregnant ddY mice (average weight, 39.5 g), and 40, 10.6, or 3.2 mg/mouse of sodium chlorate was administered to mice. Injection was performed on days 8.5 or 9.0 of gestation, which corresponds to Ed 8.5 or 9.0. The day on which the vaginal plug was observed was defined as Ed 0. At 12 or 24 hours later (Ed 9.5), migration patterns of neural crest cells and the distribution of extracellular matrix molecules were examined in treated embryos. To determine the organization of dorsal root ganglia in treated embryos, they were examined histologically and immunohistochemically at Ed 11.0 or 11.5.

TABLE 1. Primary and Secondary Antibodies

Antibody	Reactivity	Dilution	Source/Ref.
4E9R Rat monoclonal	Mouse neural crest cells	1:1	Kubota et al., 1996
Antilaminin (anti-LN) Rabbit polyclonal	Laminin (LN)	1:200	Collaborative Research
Antifibronectin (anti-FN) Rabbit polyclonal	Fibronectin (FN)	1:500	Chemicon
Antitenascin-C (anti-TN) Rabbit polyclonal	Tenascin-C (TN)	1:1000	Hasegawa et al., 1997
Antitenascin-C (anti-TN) Rat monoclonal	Tenascin-C (TN)	1:50	Koyama et al., 1996
CS-56 Mouse monoclonal	Native chondroitin sulfate (CS)	1:500	Seikagaku Corp. Avnur and Geiger, 1984
1B5 Mouse monoclonal	Unsulfated chondroitin[a]	1:50	Seikagaku Corp. Couchman et al., 1984
2B6 Mouse monoclonal	Dermatan sulfate[b] (DS)	1:100	Seikagaku Corp. Sobue et al., 1989
5D4 Mouse monoclonal	Keratan sulfate (KS)	1:500	Seikagaku Corp. Caterson et al., 1983
HK-102 Rat monoclonal	Heparan sulfate core protein (perlecan)	1:200	Seikagaku Corp. Kato et al., 1988
10E4 Mouse monoclonal	Heparan sulfate (HS)	1:200	Seikagaku Corp. David et al., 1992
40.2D6 Mouse monoclonal	Islet-1 homeobox protein	1:1	DSHB[c] Ericson et al., 1992
NR-4 Mouse monoclonal	Neurofilament 68 kDa	1:4	Boehringer Mannheim Debus et al., 1983
FITC-goat anti-rat Igs	Rat Ig G, M	1:40	American Qualex
DTAF[d]-goat anti-rat IgG	Rat IgG	1:20	Chemicon
Rhodamine-goat anti-rabbit IgG	Rabbit IgG	1:40	Cappel
FITC-goat anti-mouse Igs	Mouse Ig A, G, M	1:40	Cappel
Rhodamine-goat anti-mouse Igs	Mouse Ig A, G, M	1:40	Cappel
AMCA[e]-goat anti-rabbit IgG	Rabbit IgG	1:100	Vector

[a]The epitopes recognized by 1B5 are generated by chondroitinase ABC.
[b]The epitopes recognized by 2B6 are generated by chondroitinase B.
[c]DSHB: Developmental Studies Hybridoma Bank.
[d]DTAF: dichlorotriazinylamino.
[e]AMCA: 7-amino-4-methylcoumarin-3-acetate.

PBS or 5.0 mg α-D-xyloside (p-nitrophenyl α-D-xylopyranoside; Nakarai Tesque Inc.), α-anomer of β-D-xyloside, was used in control injection.

Three-Dimensional Image Analysis

Immunostained cryosections were image-analyzed by confocal laser scanning microscopy (MRC-500; Bio-Rad) and the use of image-analyzing software [NIH image and Spyglass Dicer (Spyglass)]. Serial optical sections of 2 μm were obtained by laser microscopy and stored in the computer system (Comos). Optical sections were subsequently processed at the same binary level (X = 100) by NIH image and reconstructed as three-dimensional images covering one somite by the image stack using Spyglass Dicer. These three-dimensional images were sliced in various directions with Spyglass Dicer to analyze the distribution of immunolabeled cells and/or materials.

ACKNOWLEDGMENTS

We thank Dr. Maya Sieber-Blum for the critical reading of this manuscript, and Dr. Yasuo Nakanishi and the members of our research group for their helpful suggestions. The 40.2D6 developed by Dr. T.M. Jessell was obtained from the Developmental Studies Hybridoma Bank maintained by The University of Iowa, Department of Biological Sciences, Iowa City, IA 52242, under contract NO1-HD-7-3263 from the NICHD. Y.K. is a research fellow of the Japanese Society for the Promotion of Science.

REFERENCES

Avnur Z, Geiger B. 1984. Immunocytochemical localization of native chondroitin-sulfate in tissues and cultured cells using specific monoclonal antibody. Cell 38:811–822.

Bronner-Fraser M. 1986. Analysis of the early stages of trunk neural crest migration in avian embryos using monoclonal antibody HNK-1. Dev Biol 115:44–55.

Caterson B, Christner JE, Baker JR. 1983. Identification of a monoclonal antibody that specifically recognizes corneal and skeletal keratan sulfate. J Biol Chem 258:8848–8854.

Couchman JR, Caterson B, Christner JE, Baker JR. 1984. Mapping by monoclonal antibody detection of glycosaminoglycans in connective tissues. Nature 307:650–652.

David G, Mei Bai X, Van Der Schueren B, Cassiman J-J, Van Den Berghe H. 1992. Developmental changes in heparan sulfate expression: in situ detection with mAbs. J Cell Biol 119:961–975.

Davies J, Lyon M, Gallagher J, Garrod D. 1995. Sulphated proteoglycan is required for collecting duct growth and branching but not nephron formation during kidney development. Development 121: 1507–1517.

Debus E, Weber K, Osborn M. 1983. Monoclonal antibodies specific for glial fibrillary acidic (GFA) protein and for each of the neurofilament triplet polypeptides. Differentiation 25:193–203.

Derby MA. 1978. Analysis of glycosaminoglycans within the extracellular environments encountered by migrating neural crest cells. Dev Biol 66:321–336.

Erickson CA, Weston JA. 1983. An SEM analysis of neural crest migration in the mouse. J Embryol Exp Morphol 74:97–118.

Erickson CA, Loring JF, Lester SM. 1989. Migratory pathways of HNK-1-immunoreactive neural crest cells in the rat embryo. Dev Biol 134:112–118.

Ericson J, Thor S, Edlund T, Jessell TM, Yamada T. 1992. Early stages of motor neuron differentiation revealed by expression of homeobox gene Islet-1. Science 256:1555–1560.

Farley JR, Nakayama G, Cryns D, Segel IH. 1978. Adenosine triphosphate sulfurylase from *penicillium chrysogenum:* equilibrium binding, substrate hydrolysis, and isotope exchange studies. Arch Bioch Biophys 185:376–390.

George EL, Georges-Labouesse EN, Patel-King RS, Rayburn H, Hynes RO. 1993. Defects in mesoderm, neural tube and vascular development in mouse embryos lacking fibronectin. Development 119:1079–1091.

Goldstein RS, Teillet M-A, Kalcheim C. 1990. The microenvironment created by grafting rostral half-somites is mitogenic for neural crest cells. Proc Natl Acad Sci USA 87:4476–4480.

Hall BK. 1988. The neural crest. London: Oxford University Press.

Hasegawa K, Yoshida T, Matsumoto K, Katsuta K, Waga S, Sakakura T. 1997. Differential expression of tenascin-C and tenascin-X in human astrocytomas. Acta Neuropathol 93:431–437.

Henion PD, Garner AS, Large TH, Weston JA. 1995. trkC-mediated NT-3 signaling is required for the early development of a subpopulation of neurogenic neural crest cells. Dev Biol 172:602–613.

Hou L, Takeuchi T. 1994. Neural crest development in reptilian embryos, studied with monoclonal antibody, HNK-1. Zool Sci 11:423–431.

Kahane N, Kalcheim C. 1994. Expression of trkC receptor mRNA during development of the avian nervous system. J Neurobiol 25:571–584.

Kalcheim C, Teillet M-A. 1989. Consequences of somite manipulation on the pattern of dorsal root ganglion development. Development 106:85–93.

Kato M, Koike Y, Suzuki S, Kimata K. 1988. Basement membrane proteoglycan in various tissues: characterization using monoclonal antibodies to the Engelbreth-Holm-Swarm mouse tumor low density heparan sulfate proteoglycan. J Cell Biol 106:2203–2210.

Kerr RSE, Newgreen DF. 1997. Isolation and characterization of chondroitin sulfate proteoglycans from embryonic quail that influence neural crest cell behavior. Dev Biol 192:108–124.

Keynes RJ, Stern CD. 1984. Segmentation in the vertebrate nervous system. Nature 310:786–789.

Keynes RJ, Stern CD. 1988. Mechanisms of vertebrate segmentation. Development 103:413–429.

Kispert A, Vainio S, Shen L, Rowitch DH, McMahon AP. 1996. Proteoglycans are required for maintenance of *Wnt-11* expression in the ureter tips. Development 122:3627–3637.

Koyama Y, Norose K, Kusubata M, Irie S, Kusakabe, M. 1996. Differential expression of tenascin in the skin during hapten-induced dermatitis. Histochem Cell Biol 106:263–273.

Krull CE, Lansford R, Gale NW, Collazo A, Marcelle C, Yancopoulos GD, Fraser SE, Bronner-Fraser M. 1997. Interactions of Eph-related receptors and ligands confer rostrocaudal pattern to trunk neural crest migration. Curr Biol 7:571–580.

Kubota Y, Morita T, Ito K. 1996. New monoclonal antibody (4E9R) identifies mouse neural crest cells. Dev Dyn 206:368–378.

Landolt RM, Vaughan L, Winterhalter KH, Zimmerman DR. 1995. Versican is selectively expressed in embryonic tissues that act as barriers to neural crest migration and axon outgrowth. Development 121:2303–2312.

Le Douarin N. 1973. A biological cell labeling technique and its use in experimental embryology. Dev Biol 30:217–222.

Le Douarin NM. 1982. The neural crest. Cambridge, UK: Cambridge University Press.

Lo L, Guillemot F, Joyner AL, Anderson DJ. 1994. MASH-1: a marker and a mutation for mammalian neural crest development. Perspect Dev Neurobiol 2:191–201.

Loring JF, Erickson CA. 1987. Neural crest cell migratory pathways in the trunk of the chick embryo. Dev Biol 121:220–236.

Morrison-Graham K, Weston JA. 1989. Mouse mutants provide new insights into the role of extracellular matrix in cell migration and differentiation. Trends Genet 5:116–121.

Morriss-Kay GM, Crutch B. 1982. Culture of rat embryos with β-D-xyloside: evidence of a role for proteoglycans in neurulation. J Anat 134:491–506.

Newgreen DF, Powell ME, Moser B. 1990. Spatiotemporal changes in HNK-1/L2 glycoconjugates on avian embryo somite and neural crest cells. Dev Biol 139:100–120.

Oakley RA, Tosney KW. 1991. Peanut agglutinin and chondroitin-6-sulfate are molecular markers for tissues that act as barriers to axon advance in the avian embryo. Dev Biol 147:187–206.

Oike Y, Kimata K, Shinomura T, Nakazawa K, Suzuki S. 1980. Structural analysis of chick-embryo cartilage proteoglycan by selective degradation with chondroitin lyases (chondroitinases) and endo-β-D-galactosidase (keratanase). Biochem J 191:193–207.

Okayama M, Kimata K, Suzuki S. 1973. The influence of *p*-nitrophenyl β-D-xyloside on the synthesis of proteochondroitin sulfate by slices of embryonic chick cartilage. J Biochem 74:1069–1073.

Oohira A, Nogami H, Nakanishi Y. 1981. Abnormal overgrowth of chick embryos treated with p-nitrophenyl β-D-xyloside at early stages of development. J Embryol Exp Morphol 61:221–232.

Perris R, Krotoski D, Lallier T, Domingo C, Sorrell JM, Bronner-Fraser M. 1991. Spatial and temporal changes in the distribution of proteoglycans during avian neural crest development. Development 111:583–599.

Perris R, Perissinotto D, Pettway Z, Bronner-Fraser M, Mörgelin M, Kimata K. 1996. Inhibitory effects of PG-H/aggrecan and PG-M/versican on avian neural crest migration. FASEB J 10:293–301.

Rickmann M, Fawcett JW, Keynes RJ. 1985. The migration of neural crest cells and the growth of motor axons through the rostral half of the chick somite. J Embryol Exp Morphol 90:437–455.

Schuchardt A, D'Agati V, Larsson-Blomberg L, Costantini F, Pachnis V. 1994. Defects in the kidney and enteric nervous system of mice lacking the tyrosine kinase receptor Ret. Nature 367:380–383.

Schwartz NB. 1977. Regulation of chondroitin sulfate synthesis: effect of β-D-xylosides on synthesis of chondroitin sulfate proteoglycan, chondroitin sulfate chains, and core protein. J Biol Chem 252:6316–6321.

Schwartz NB, Galligani L, Ho P-L, Dorfman A. 1974. Stimulation of synthesis of free chondroitin sulfate chains by β-D-xylosides in cultured cells. Proc Natl Acad Sci USA 71:4047–4051.

Serbedzija GN, Bronner-Fraser M, Fraser SE. 1989. A vital dye analysis of the timing and pathways of avian trunk neural crest cell migration. Development 106:809–816.

Serbedzija GN, Fraser SE, Bronner-Fraser M. 1990. Pathways of trunk neural crest cell migration in the mouse embryo as revealed by vital dye labelling. Development 108:605–612.

Silvers WK. 1979. The coat colors of mice. New York: Springer-Verlag.

Sobue M, Takeuchi J, Fukatsu T, Nagasaka T, Nakashima N, Ogura T, Katoh T, Yoshida K. 1989. Immunohistochemical techniques for detection of dermatan sulfate proteoglycan in tissue sections. Stain Technol 64:43–47.

Sternberg J, Kimber SJ. 1986. The relationship between emerging neural crest cells and basement membranes in the trunk of the mouse embryo: a TEM and immunocytochemical study. J Embryol Exp Morphol 98:251–268.

Tan S-S, Crossin KL, Hoffman S, Edelman GM. 1987. Asymmetric expression in somites of cytotactin and its proteoglycan ligand is correlated with neural crest cell distribution. Proc Natl Acad Sci USA 84:7977–7981.

Tosney KW, Dehnbostel DB, Erickson CA. 1994. Neural crest cells prefer the myotome's basal lamina over the sclerotome as a substratum. Dev Biol 163:389–406.

Trasler DG, Morriss-Kay G. 1991. Immunohistochemical localization of chondroitin and heparan sulfate proteoglycans in pre-spina bifida splotch mouse embryos. Teratology 44:571–579.

Wang HU, Anderson DJ. 1997. Eph family transmembrane ligands can mediate repulsive guidance of trunk neural crest migration and motor axon outgrowth. Neuron 18:383–396.

Wehrle-Haller B, Weston JA. 1995. Soluble and cell-bound forms of steel factor activity play distinct roles in melanocyte precursor dispersal and survival on the lateral neural crest migration pathway. Development 121:731–742.

Wehrle-Haller B, Weston JA. 1997. Receptor tyrosine kinase-dependent neural crest migration in response to differentially localized growth factors. BioEssays 19:337–345.

Weston JA. 1963. A radioautographic analysis of the migration and localization of trunk neural crest cells in the chick. Dev Biol 6:279–310.

Weston JA. 1970. The migration and differentiation of neural crest cells. Adv Morphogen 8:41–114.

Weston JA, Pintar JE, Derby MA, Nichols DH. 1977. The morphogenesis of spinal ganglia from neural crest cells. In: Hall Z, Kelly R, Fox C, editors. Progress in clinical and biological research. New York: Alan R. Liss, p 217–226.

Yada T, Koide N, Kimata K. 1996. Transient accumulation of perisinusoidal chondroitin sulfate proteoglycans during liver regeneration and development. J Histochem Cytochem 44:969–980.